Biochemical and Biophysical Research Communications 404 (2011) 245–249

Contents lists available at ScienceDirect

Biochemical and Biophysical Research Communications

journal homepage: www.elsevier.com/locate/ybbrc

The crystal structure of a *Thermus thermophilus* $tRNA^{Gly}$ acceptor stem microhelix at 1.6 Å resolution

D. Oberthür [a], A. Eichert [b], V.A. Erdmann [b], J.P. Fürste [b], Ch. Betzel [a], C. Förster [b,*]

[a] Institute of Biochemistry and Molecular Biology, Laboratory for Structural Biology of Infection and Inflammation, University of Hamburg, c/o DESY, 22603 Hamburg, Germany
[b] Institute of Chemistry and Biochemistry, Free University Berlin, Thielallee 63, 14195 Berlin, Germany

ARTICLE INFO

Article history:
Received 22 November 2010
Available online 27 November 2010

Keywords:
Thermus thermophilus $tRNA^{Gly}$ acceptor stem microhelix
Crystal structure
tRNA identity elements
Glycyl-tRNA synthetase (GlyRS)
RNA hydration

ABSTRACT

tRNAs are aminoacylated with the correct amino acid by the cognate aminoacyl-tRNA synthetase. The tRNA/synthetase systems can be divided into two classes: class I and class II. Within class I, the tRNA identity elements that enable the specificity consist of complex sequence and structure motifs, whereas in class II the identity elements are assured by few and simple determinants, which are mostly located in the tRNA acceptor stem.

The $tRNA^{Gly}$/glycyl-tRNA-synthetase (GlyRS) system is a special case regarding evolutionary aspects. There exist two different types of GlyRS, namely an archaebacterial/human type and an eubacterial type, reflecting the evolutionary divergence within this system. We previously reported the crystal structures of an *Escherichia coli* and of a human $tRNA^{Gly}$ acceptor stem microhelix. Here we present the crystal structure of a thermophilic $tRNA^{Gly}$ aminoacyl stem from *Thermus thermophilus* at 1.6 Å resolution and provide insight into the RNA geometry and hydration.

1. Introduction

The genetic code consists of 64 codons that have to be translated into protein. tRNAs translate the information by transporting the corresponding amino acid to the ribosome, where the protein biosynthesis takes place. There are 20 natural amino acids, which implicates that the genetic code is redundant. tRNA isoacceptors enable the translation of different mRNA triplets that code for the same amino acid. tRNA identity elements assure the correct aminoacylation of tRNA with the cognate amino acid by the specific aminoacyl-tRNA synthetases. In the so called class II system, the tRNA determinants consist of rather few and simple sequence and structure motifs, which are mainly located in the aminoacyl stem of the tRNA [1]. The $tRNA^{Gly}$/glycyl-tRNA synthetase (GlyRS) belongs to the class II system. The $tRNA^{Gly}$ identity elements consist of sequence motifs in the aminoacyl stem and additionally of the discriminator base at position 73 [2,3].

Within the glycine system, a large difference can be described regarding the synthetase substructures between eukaryotes/archaebacteria and eubacteria. This is a special case within tRNA/synthetase systems and possibly represents an evolutionary divergence. The eukaryotic/archaebacterial glycine system and the eubacterial system differs not only in the protein structure, but also in the respective tRNA identity elements. This system has been thoroughly investigated within different organisms and a number of GlyRS sequences are published up to now, like the protein from the baker's yeast [4], the silkworm *Brombix mori* [5] and human [3,6]. The eukaryotic/archaebacterial GlyRS possesses the α_2 structure and recognizes the tRNA aminoacyl stem with the discriminator base A73.

On the contrary, the eubacterial GlyRS consists of an $\alpha_2\beta_2$ structure and also recognizes tRNA determinants in the acceptor stem, but the discriminator base has strictly to be an U73 instead of an A73. Additionally, a strong sequence divergence of the protein motifs 1–3 is reported, which is usually highly conserved among class II aminoacyl-tRNA-synthetases [1,6]. As example, the GlyRS from *Escherichia coli* is a tetrameric protein and consists of the $\alpha_2\beta_2$ structure [7,8] with both subunits being responsible for the enzymatic activity [7]. The α-subunit is responsible for ATP- and glycine-binding and thus for amino acid activation, whereas the β-subunit is the part, which binds to the $tRNA^{Gly}$ [9–11]. In this case, the $tRNA^{Gly}$ identity elements are built up of the conserved base pair C2-G71 and of the U73 discriminator base [2].

Regarding the $tRNA^{Gly}$/GlyRS of the eubacterium *Thermus thermophilus*, the system becomes even more complex. A 2.75 Å crystal structure of the *T. thermophilus* GlyRS [12] could demonstrate that the enzyme surprisingly represents the structure that can rather be brought in vicinity to the eukaryotic/archaebacterial type, but the enzyme depends on the eubacterial $tRNA^{Gly}$ identity elements.

We focussed our interest on high resolution crystal structures of $tRNA^{Gly}$ microhelices to contribute to the understanding of the $tRNA^{Gly}$/GlyRS structure diversity within eu- and archaebacterial

* Corresponding author. Fax: +49 30 838 56413.
E-mail address: foerster@chemie.fu-berlin.de (C. Förster).

0006-291X/$ - see front matter © 2010 Elsevier Inc. All rights reserved.
doi:10.1016/j.bbrc.2010.11.101

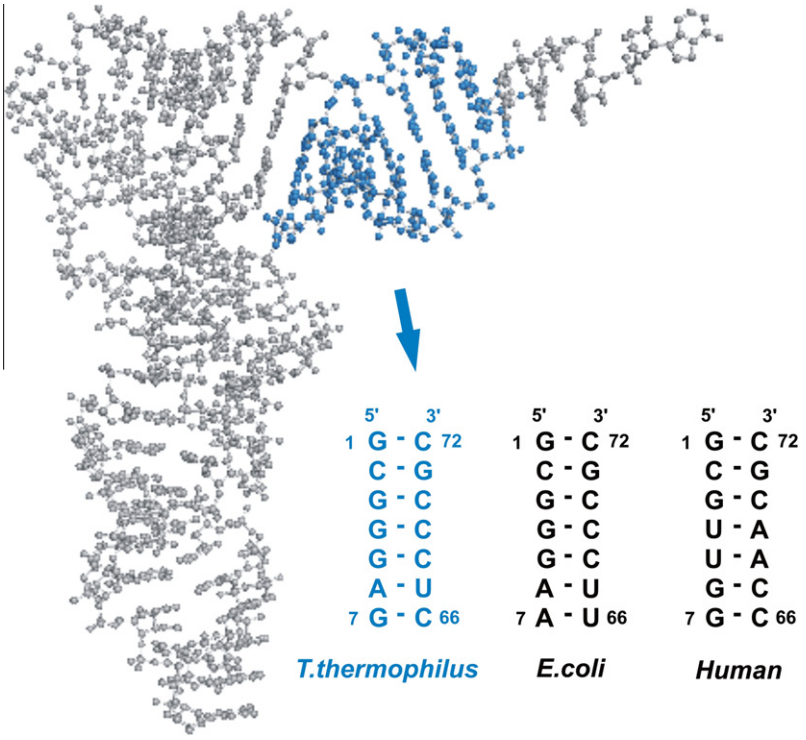

Fig. 1. The tRNA tertiary structure with the aminoacyl stem highlighted in blue. The sequence of the *T. thermophilus* $tRNA^{Gly}$ microhelix, which was investigated in this study, is pointed out in blue. The two other sequences in black represent the sequences of the previously solved $tRNA^{Gly}$ microhelix structures from *E. coli* and human. (For interpretation of the references to colour in this figure legend, the reader is referred to the web version of this article.)

Table 1
X-ray diffraction data and refinement statistics of the *T. thermophilus* $tRNA^{Gly}$ microhelix crystal.

Space group	*P*1
Cell edges (Å)	$a = 26.19$, $b = 29.02$, $c = 29.53$
Cell angles (°)	$\alpha = 107.17$, $\beta = 97.37$, $\gamma = 96.55$
Radiation source	DESY/HASYLAB/consortiums beam line X13
Wavelength (Å)	0.8123
Resolution range (Å)	36.0–1.60
No. of total reflections	34,624
No. of unique observations	10,142
Completeness (%)	94.7 (72.9)
Multiplicity[a]	3.4 (2.1)
Average $I/\sigma(I)$[a,b]	14.5 (1.7)
R_{merge}[a,c] (%)	6.6 (35.4)
Molecules per asymmetric unit	2
Matthews coefficient (Å^3/Da)	2.52
Water content (%)[d]	62.59
Final R/R_{free} (%)[e]	23.7/28.0
RNA atoms	588
Water oxygen atom loci	88
Rmsd bond lengths (Å)[f]	0.025
Rmsd angles (°)[f]	3.14

[a] Values for the resolution shell 36.0–1.60 Å and in parenthesis for the highest resolution shell 1.63–1.60 Å.
[b] Reflection intensity.
[c] $R_{merge} = \sum_{hkl} \sum_i |I_i(hkl) - \langle I(hkl)\rangle| / \sum_{hkl} \sum_i I_i(hkl)$, where $I_i(hkl)$ and $\langle I(hkl)\rangle$ are the observed individual and mean intensities of a reflection with the indices *hkl*, respectively, $\sum_i$ is the sum over the individual measurements of a reflection with the indices *hkl*, and $\sum_{hkl}$ is the sum over all reflections.
[d] Calculated by considering the standard atomic volumes for RNA according to [30].
[e] R_{free} = based on 5% of the data selected with *REFMAC5* [25,26].
[f] Rmsd: root-mean-square deviation.

systems. Recently, we presented the structures of an *E. coli* $tRNA^{Gly}$ microhelix at 2.0 Å [13], a human $tRNA^{Gly}$ acceptor stem at 1.2 Å resolution [14] and a comparison between both structures [15]. Now we solved the structure of the *T. thermophilus* $tRNA^{Gly}$ acceptor stem microhelix at a resolution of 1.6 Å. With this structure, we wish to contribute to the general understanding of tRNA identity elements [16–19] and help to further interpret the $tRNA^{Gly}$/GlyRS system with special focus on the unusual *T. thermophilus* system.

2. Materials and methods

2.1. Crystallization of the T. thermophilus $tRNA^{Gly}$ microhelix

The $tRNA^{Gly}$ acceptor stem from *T. thermophilus* was adapted from the tRNA sequence compilation and possesses the sequence 5′-$G_1C_2G_3G_4G_5A_6G_7$-3′/5′-$C_{66}U_{67}C_{68}C_{69}C_{70}G_{71}C_{72}$-3′ [20] and corresponds to the tRNA isoacceptor number RG 1580. The numbering corresponds to the canonical tRNA convention. Crystals with maximum dimensions of $0.1 \times 0.2 \times 0.2$ mm were grown using the hanging drop vapour diffusion technique with 1 µl 40 mM sodium cacodylate, pH 7.0, 12 mM spermine tetra-HCl, 80 mM NaCl and 10% (v/v) MPD (2-methyl-2,4-pentanediol) as precipitant solution that was mixed with 1 µl 0.5 mM RNA and equilibrated against 1 ml 35% (v/v) MPD at 21 °C. The crystals were flash-frozen in liquid nitrogen prior to data collection without using any further cryo-protecting reagent.

2.2. Acquisition of X-ray diffraction data

The X-ray diffraction data were collected at the DESY/HASYLAB consortiums beam line X13 in Hamburg (Germany). A data set from 36.0 to 1.60 Å was recorded at a wavelength of 0.8123 Å and a temperature of 100 K. Crystallographic data processing was performed using the programs *DENZO* and *SCALEPACK* from the *HKL*-2000 suite [21]. For a merohedral twinning analysis, the data were applied to the Padilla and Yeates algorithm [22], as implemented in the web server http://nihserver.mbi.ucla.edu/pystats.

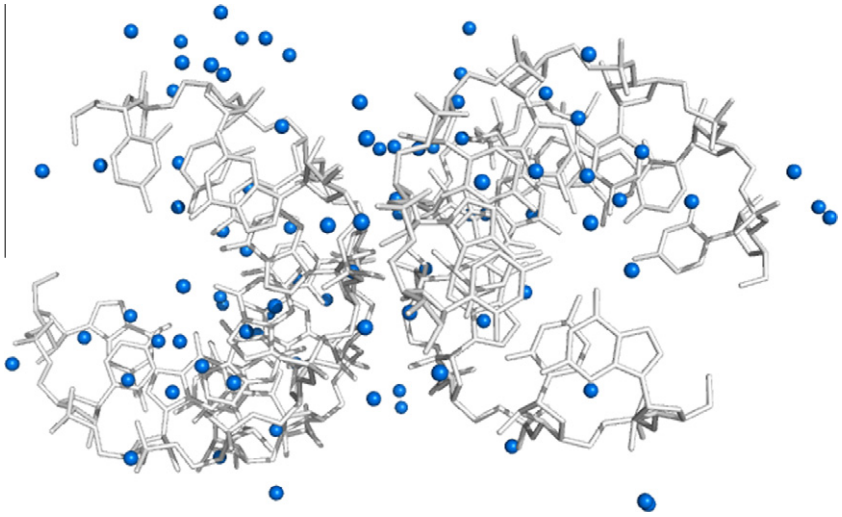

Fig. 2. Crystal packing of the *T. thermophilus* $tRNA^{Gly}$ microhelix showing the orientation of the two RNA helices per asymmetric unit. The water molecules, 88 in total, are presented as blue dots. (For interpretation of the references to colour in this figure legend, the reader is referred to the web version of this article.)

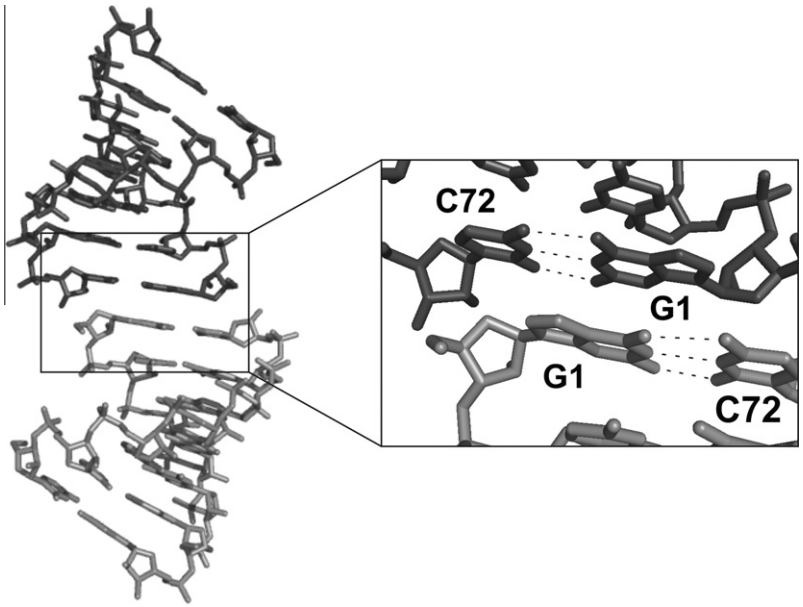

Fig. 3. Crystal packing of the *T. thermophilus* $tRNA^{Gly}$ microhelix showing the stacking behaviour of the RNA duplexes. The two RNA molecules are presented in dark and light grey. The RNAs form endless helices in the crystal structure (left picture). The stacking is favored by hydrophobic inter-strand interactions between the first guanosine residues (G1) of two helices, which stack in a 'head-to-head' manner (highlighted in the right picture).

2.3. Structure determination and refinement

The structure of the *T. thermophilus* $tRNA^{Gly}$ acceptor stem microhelix could be solved by using molecular replacement techniques. As a model, we constructed an artificial $tRNA^{Gly}$ microhelix with corresponding nucleotide sequence by using the program *COOT* [23]. This artificial duplex was used after routinely checking the standard RNA geometry and the correct base pair distances without using further calculations or structure optimizations. Molecular replacement was calculated with the program *PHASER* [24] as implemented in the *CCP4i*-package (Collaborative Computational Project, Number 4) [25]. All structure data were refined with *REFMAC5* [26] and electron maps were calculated with *FFT* [27]. The programs *COOT* [23] and *PYMOL* [28] were used for visualization and building of the RNA. Calculation of average and local helical parameters was done with the program *X3DNA* [29]. The coordinates of the *T. thermophilus* $tRNA^{Gly}$ acceptor stem microhelix structure have been deposited at the RSCB protein data bank with the PDB ID: 2XSL.

3. Results and discussion

3.1. Crystallographic data, overall and local geometric parameters of the T. thermophilus $tRNA^{Gly}$ microhelix

The *T. thermophilus* $tRNA^{Gly}$ acceptor stem microhelix isoacceptor RG 1580 [20] with the sequence 5′-$G_1C_2G_3G_4G_5A_6G_7$-3′/5′-$C_{66}U_{67}C_{68}C_{69}C_{70}G_{71}C_{72}$-3′ (Fig. 1) was crystallized and the X-ray structure was solved to 1.6 Å resolution. Molecular replacement calculations using an artificially constructed RNA duplex with the sequence corresponding to the *T. thermophilus* $tRNA^{Gly}$ microhelix lead to a successful structure determination. The 7-mer helix

Table 2
Selected local helical parameters of the *T. thermophilus* tRNA^{Gly} acceptor stem microhelix. Molecules A and B represent the two RNA helices per asymmetric unit.

	Twist (°)	Slide (Å)	Tilt (°)	Rise (Å)	Prop. twist (°)
Molecule A					
G1-C72	32.05	−1.89	−1.68	2.59	−4.00
C2-G71	32.27	−1.75	0.75	2.68	−9.04
G3-C70	32.05	−1.60	−1.97	2.72	−9.48
G4-C69	31.45	−1.71	3.62	2.65	−10.47
G5-C68	34.10	−1.20	1.40	2.56	−14.80
A6-U67	32.69	−1.63	0.19	2.70	−11.91
G7-C66					−12.18
Molecule B					
G1-C72	32.43	−1.64	−1.61	2.77	−5.88
C2-G71	32.12	−1.76	2.35	2.63	−11.66
G3-C70	31.49	−1.75	−0.57	2.65	−10.29
G4-C69	30.31	−1.81	0.47	2.71	−4.24
G5-C68	35.16	−1.56	0.99	2.63	−13.25
A6-U67	31.79	−1.73	0.61	2.76	−8.54
G7-C66					−11.12

crystallizes in the space group *P*1 with two molecules per asymmetric unit and the following cell constants: $a = 26.19$, $b = 29.02$, $c = 29.53$ Å and $\alpha = 107.17$, $\beta = 97.37$, $\gamma = 96.55°$ (Table 1). We calculated a Matthews coefficient of 2.52 Å^3/Da, which corresponds to a solvent content of 62.59% by considering the standard atomic volumes of RNA according to Voss and Gerstein [30]. There are 588 RNA atoms per asymmetric unit and a total of 88 water oxygen atoms (Fig. 2). The data were refined to the final *R*-values of $R/R_{free} = 23.7/28.0\%$ (Table 1). The RNA molecules form so called 'endless helices' within the crystal lattice by stacking onto each other in a 'head to head' manner. This kind of packing is favored by hydrophobic inter-strand interactions between the first guanosine nucleotides of both strands (Fig. 3).

Insight into selected local helical parameters of the two tRNA^{Gly} microhelices per asymmetric unit is given in Table 2. All data show values reflecting a canonical A-type RNA helix. The phosphate backbone α/γ torsion angles all adopt the (−) gauche/(+) gauche conformation, while the β torsion angles show the anti conformation around ±180° and do not deviate from the canonical A-form RNA (data not shown). We recently reported the structures of tRNA^{Gly} microhelices from *E .coli* and from human [13,14]. Further, a comparative analysis between these structures has been undertaken by superposition experiments [15]. As expected, the average helical parameters of the human tRNA^{Gly} microhelix and the *E. coli* tRNA^{Gly} microhelix possess the overall A-type RNA geometry, but differences could be detected within the solvent distribution. We will now undertake superposition experiments of the *T. thermophilus* tRNA^{Gly} microhelix with the *E. coli* and the human microhelix focussing on the thermophilic origin of the here reported tRNA. The *T. thermophilus* tRNA^{Gly} acceptor stem microhelix possesses six CG pairs and one AU pair and the GC-rich sequence should be the main reason for the thermostability. Nevertheless, further comparative structure investigations between the tRNA^{Gly} microhelices from *T. thermophilus*, *E. coli* and human are underway with special interest regarding the RNA hydration patterns.

3.2. The hydration pattern of the T. thermophilus tRNA^{Gly} microhelix

The 1.6 Å crystal structure of the *T. thermophilus* tRNA^{Gly} microhelix allows identification of defined water oxygen atoms and provides a detailed description of their position within the RNA structure. We detected a total of 88 water molecules within the two RNA molecules per asymmetric unit. The structure is not completely saturated by water molecules. It is conceivable that, despite a resolution of 1.6 Å, several solvent molecules are not visible in the electron density map. Nevertheless, we could detect several regions in the *T. thermophilus* tRNA^{Gly} microhelix that show a nearby complete saturation with water molecules. One example is displayed for the base pair G3-C70 in Fig. 4. Water molecules are associated to the endocyclic nitrogen of the G3 and to the oxygen atom of the phosphate in the major groove. Additionally, a water molecule is in vicinity of the exocyclic aminogroup at position 4 of the C70 and a second water molecule contacts the phosphate of this nucleotide. In the minor groove, we detect solvent molecules contacting the exocyclic aminogroup of the G3. Another water is associated to the endocyclic nitrogen of the guanosine and is in contact to the 2′-hydroxyl group of the ribose. Regarding the C70, we also detect a water molecule in vicinity to the ribose 2′-OH group. Altogether, the water molecules build a tight network surrounding the base pairs and provide a hydration layer of the RNA. It is well accepted that the hydration of RNA plays an important role in RNA–protein interactions and that the extensive solvent content of the minor groove has a special function in RNA [31,32]. We will thus further focus on the comparison of the hydration patterns in the tRNA^{Gly} microhelices from *T. thermophilus*, *E. coli* and human (in preparation).

The unusual divergence between the human/archaebacterial and the eubacterial tRNA^{Gly}/GlyRS system opens questions,

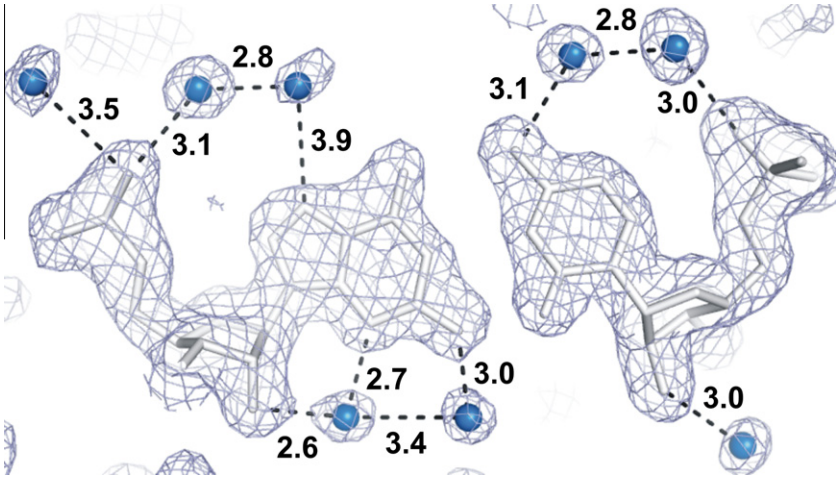

Fig. 4. $2F_o - F_c$ electron density map at 1.6 Å resolution showing the base pair G3-C70 of the *T. thermophilus* tRNA^{Gly} microhelix. Water molecules are shown as blue dots and distances are indicated in Å. (For interpretation of the references to colour in this figure legend, the reader is referred to the web version of this article.)

whether there are structural differences within the tRNAs in general and within the acceptor stems in special, as this part carries the identity elements in $tRNA^{Gly}$ [2,3]. We began with structure determination and comparative analysis of *E. coli* and human $tRNA^{Gly}$ microhelices [13–15] and now complement these investigations with the $tRNA^{Gly}$ microhelix structure from *T. thermophilus*. A further comparative structure investigation by undertaking superposition experiments of the helices and the hydration patterns of all three $tRNA^{Gly}$ microhelices is in progress.

Acknowledgments

This work was supported by the BiGRUDI network of the Robert Koch Institute (Berlin) financed by the Bundesministerium für Bildung und Forschung. AE is member of the Dahlem Research School of the Free University Berlin and funded by the Friedrich-Ebert-Stiftung, Germany. We gratefully acknowledge the DESY synchrotron, Hamburg, Germany for providing beam time.

References

[1] G. Eriani, M. Delarue, O. Poch, J. Gangloff, D. Moras, Partition of tRNA synthetases into two classes based on mutually exclusive sets of sequence motifs, Nature 347 (1990) 203–206.
[2] W.H. McClain, K. Foss, R.A. Jenkins, J. Schneider, Rapid determination of nucleotides that define tRNA(Gly) acceptor identity, Proc. Natl. Acad. Sci. USA 88 (1991) 6147–6151.
[3] K. Shiba, P. Schimmel, H. Motegi, T. Noda, Human glycyl-tRNA synthetase. Wide divergence of primary structure from bacterial counterpart and species-specific aminoacylation, J. Biol. Chem. 269 (1994) 30049–30055.
[4] D. Kern, R. Giege, J.P. Ebel, Glycyl-tRNA synthetase from baker's yeast. Interconversion between active and inactive forms of the enzyme, Biochemistry 20 (1981) 122–131.
[5] S. Nada, P.K. Chang, J.D. Dignam, Primary structure of the gene for glycyl-tRNA synthetase from *Bombyx mori*, J. Biol. Chem. 268 (1993) 7660–7667.
[6] K. Shiba, The Aminoacyl-tRNA Synthetases, Landess Bioscience, Georgetown, Texas, USA, 2005 (Chapter 13).
[7] D.L. Ostrem, P. Berg, Glycyl transfer ribonucleic acid synthetase from *Escherichia coli*: purification, properties, and substrate binding, Biochemistry 13 (1974) 1338–1348.
[8] T.A. Webster, B.W. Gibson, T. Keng, K. Biemann, P. Schimmel, Primary structures of both subunits of *Escherichia coli* glycyl-tRNA synthetase, J. Biol. Chem. 258 (1983) 10637–10641.
[9] G.M. Nagel, S. Cumberledge, M.S. Johnson, E. Petrella, B.H. Weber, The beta subunit of *E. coli* glycyl-tRNA synthetase plays a major role in tRNA recognition, Nucl. Acids Res. 12 (1984) 4377–4384.
[10] M.J. Toth, P. Schimmel, Deletions in the large (beta) subunit of a hetero-oligomeric aminoacyl-tRNA synthetase, J. Biol. Chem. 265 (1990) 1000–1004.
[11] M.J. Toth, P. Schimmel, A mutation in the small (alpha) subunit of glycyl-tRNA synthetase affects amino acid activation and subunit association parameters, J. Biol. Chem. 265 (1990) 1005–1009.
[12] D.T. Logan, M.H. Mazauric, D. Kern, D. Moras, Crystal structure of glycyl-tRNA synthetase from *Thermus thermophilus*, EMBO J. 14 (1995) 4156–4167.
[13] C. Förster, A.B. Brauer, M. Perbandt, D. Lehmann, J.P. Fürste, C. Betzel, V.A. Erdmann, Crystal structure of an *Escherichia coli* tRNA(Gly) microhelix at 2.0 Å resolution, Biochem. Biophys. Res. Commun. 363 (2007) 621–625.
[14] C. Förster, M. Mankowska, J.P. Fürste, M. Perbandt, C. Betzel, V.A. Erdmann, Crystal structure of a human tRNA(Gly) microhelix at 1.2 Å resolution, Biochem. Biophys. Res. Commun. 368 (2008) 996–1001.
[15] C. Förster, A. Zerressen-Harte, J.P. Fürste, M. Perbandt, C. Betzel, V.A. Erdmann, Comparative X-ray structure analysis of human and *Escherichia coli* tRNA(Gly) acceptor stem microhelices, Biochem. Biophys. Res. Commun. 368 (2008) 1002–1006.
[16] S. Limmer, H.P. Hofmann, G. Ott, M. Sprinzl, The 3′-terminal end (NCCA) of tRNA determines the structure and stability of the aminoacyl acceptor stem, Proc. Natl. Acad. Sci. USA 90 (1993) 6199–6202.
[17] U. Mueller, H. Schubel, M. Sprinzl, U. Heinemann, Crystal structure of acceptor stem of tRNA(Ala) from *Escherichia coli* shows unique G.U wobble base pair at 1.16 Å resolution, RNA 5 (1999) 670–677.
[18] A. Ramos, G. Varani, Structure of the acceptor stem of *Escherichia coli* tRNA Ala: role of the G3.U70 base pair in synthetase recognition, Nucl. Acids Res. 25 (1997) 2083–2090.
[19] M. Seetharaman, C. Williams, C.J. Cramer, K. Musier-Forsyth, Effect of G-1 on histidine tRNA microhelix conformation, Nucl. Acids Res. 31 (2003) 7311–7321.
[20] M. Sprinzl, K.S. Vassilenko, Compilation of tRNA sequences and sequences of tRNA genes, Nucl. Acids Res. 33 (2005) D139–D140.
[21] Z. Otwinowski, W. Minor, Processing of X-ray Diffraction Data Collected in Oscillation Mode, Methods Enzymol. Macromol. Crystallogr. Part A (1997) 276–307.
[22] J.E. Padilla, T.O. Yeates, A statistic for local intensity differences: robustness to anisotropy and pseudo-centering and utility for detecting twinning, Acta Crystallogr. D 59 (2003) 1124–1130.
[23] P. Emsley, K. Cowtan, Coot: model-building tools for molecular graphics, Acta Crystallogr. D Biol. Crystallogr. 60 (2004) 2126–2132.
[24] A.J. McCoy, R.W. Grosse-Kunstleve, L.C. Storoni, R.J. Read, Likelihood-enhanced fast translation functions, Acta Crystallogr. D. Biol. Crystallogr. 61 (2005) 458–464.
[25] Collaborative Computational Project, Number 4, "The CCP4 Suite: Programs for Protein Crystallography", Acta Crystallogr. D 50 (1994) 760–763.
[26] G.N. Murshudov, A.A. Vagin, E.J. Dodson, Refinement of macromolecular structures by the maximum-likelihood method, Acta Crystallogr. D. Biol. Crystallogr. 53 (1997) 240–255.
[27] R.J. Read, A.J. Schierbeek, A phased translation function, J. Appl. Cryst. 21 (1988) 490–495.
[28] L. Warren, The PyMOL Molecular Graphics System De Lano Scientific LCC, San Carlos, CA, USA, 2005.
[29] X.J. Lu, W.K. Olson, 3DNA: a software package for the analysis, rebuilding and visualization of three-dimensional nucleic acid structures, Nucl. Acids Res. 31 (2003) 5108–5121.
[30] N.R. Voss, M. Gerstein, Calculation of standard atomic volumes for RNA and comparison with proteins: RNA is packed more tightly, J. Mol. Biol. 346 (2005) 477–492.
[31] P. Auffinger, E. Westhof, Hydration of RNA base pairs, J. Biomol. Struct. Dyn. 16 (1998) 693–707.
[32] D.E. Draper, Themes in RNA-protein recognition, J. Mol. Biol. 293 (1999) 255–270.